ISLAMIC AZAD UNIVERSITY MARVDASHT BRANCH

Journal of Land Use and Sustainable Development

Autumn & winter 2024. Vol 1. Issue 1

E-ISSN: 3092-6785

https://sanad.iau.ir/journal/jlusd

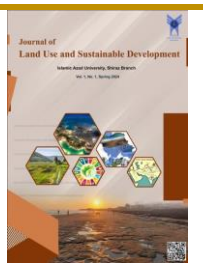

Original Research Paper

From Theory to Practice: Implementing PVsyst Modeling for Solar Power Plant Design, (case study of Iran)

Farshad Rafipour*: Professor in Department of Urban Planning, North Tehran Branch, Islamic Azad University, Tehran, Iran.

Narges Nonejad: Ph.D. in Department of Urban Planning, North Tehran Branch, Islamic Azad University, Tehran, Iran.

ARTICLE INFO

Received: 2024/11/24
Accepted: 2025/02/20
PP: 53-70

Use your device to scan and read the article online

Keywords: *Location, Solar Power Plant, Tonekabon, IHWP Method, PVsyst Method*

Abstract

The increasing focus on renewable energy sources presents a viable alternative to non-renewable fossil fuels, with solar energy gaining particular attention. This research aims to identify and zone areas suitable for the construction of solar power plants in the neighborhoods of Islamabad and Shiroodi in Tonekabon city. This applied research employs a descriptive-analytical method. The study's statistical population consists of 30 experts in the field, from which 28 were selected as the sample using the Cochran formula. Data collection methods included questionnaires, field observations, and documentary studies. The data analysis for determining solar power plant locations utilized the IHWP (Inverse Hierarchy Analysis) method within GIS software, along with PVsyst modeling for rooftop and ground-mounted power plants.The research findings indicate that 26% of the city area is classified as very unsuitable for solar development, 23% as unsuitable, 20% as relatively suitable, 20% as suitable, and 11% as completely suitable, with the most favorable areas located primarily in the central part of the city. The Islamabad neighborhood shows greater potential for solar power plant construction, with 72.88% of its central area deemed suitable, compared to 27.11% in the southern area of Shiroodi. Specifically, identification code 54 in the Shiroodi neighborhood ranks first for suitability, while identification codes 26 and 27 in the Islamabad neighborhood follow in second place.

Citation: Rafipour, F., & Nonejad, N. (2024). **From Theory to Practice: Implementing PVsyst Modeling for Solar Power Plant Design, a case study of Iran**. *Journal of Land Use and Sustainable Development*, 1(1), 53-70.

DOI: 10.82173/jlusd.2025.1207006

COPYRIGHTS

©2023 The author(s). This is an open access article distributed under the terms of the Creative Commons Attribution (CC BY 4.0), which permits unrestricted use, distribution, and reproduction in any medium, as long as the original authors and source are cited. No permission is required from the authors or the publishers.

OPEN ACCESS

* **Corresponding author:** Farshad Rafipour **Email:** far_raf2004@yahoo.com **Tel:** +98911 856 4814

INTRODUCTION

Energy is a crucial driver of economic growth and societal development, particularly for nations that utilize it efficiently. Conversely, countries that consume less energy are often regarded as economically disadvantaged (Khajavipour et al, 2021). The rising need for renewable energy has led to increased demand for solar energy, positioning it as a viable alternative to non-renewable fossil fuels and prompting societies to adopt solar technologies (Wei, Islam, Hasanuzzaman, & Cuce, 2024). Given the universal demand for electrical energy, various methods exist to produce it with minimal environmental impact, among which solar energy stands out (Rana & Moniruzzaman, 2024). Solar energy is one of the most accessible and cleanest resources, requiring relatively simple and cost-effective technology for harnessing (Hassaan, Hassan, & Al-Dashti, 2021).

Research into urban thermal performance is vital, aiming to lower energy consumption, cut carbon emissions, and promote sustainable energy sources (Alghoul et al, 2017). With advancements in technology and the political commitment of both developed and developing nations, along with a focus on resilience and sustainable development, assessing the potential of renewable energies has become a key aspect of energy policies and urban planning. This includes strategies to reduce reliance on fossil fuels, minimize carbon footprints, and enhance the use of renewable energy (Nandini et al, 2024).

Energy demands vary based on climate, energy technologies, and urban design, influencing the placement of solar panels and overall energy consumption (Ahmadian, 2021). There are opportunities to enhance sustainability in certain areas through modern tools like Geographic Information Systems (GIS), which enable effective spatial analysis (Hassaan et al., 2021). GIS-based multi-criteria decision-making methods are increasingly employed in urban planning and spatial management (Zhang, Xu, & Liu, 2024).

Iran boasts significant solar energy potential, with over 300 sunny days across much of the country and an average solar radiation of 4.5-5.5 kWh/m²/day (Ajiboye, Agboola, Atayese, & Kadiri, 2011). Tonekabon, located in Mazandaran province, particularly in the neighborhoods of Shiroodi and Islamabad, benefits from 800 hours of sunshine annually, making it well-suited for renewable energy applications. Analyzing this region's geographical features suggests that solar renewable energies could significantly enhance energy efficiency, provided that solar power plants and photovoltaic panels are strategically located.

Solar energy technologies are recognized as pivotal solutions for producing clean and renewable energy globally. Photovoltaic (PV) technologies convert sunlight into electricity using solar panels, and their adoption has surged in recent years. According to the International Energy Agency (IEA), global solar panel installations exceeded 600 GW in 2020, with expectations for continued growth. Moreover, technological advancements have led to substantial decreases in solar PV production costs, making it a preferred option in many countries (Kumar, Rajoria, Sharma, & Suhag, 2021).

Main Objective: To zone and simulate the construction of a solar power plant in the coastal city of Tonekabon using the IHWP and PV sys methods.

Main Question: Which locations in the study area are most suitable for establishing solar power plants and photovoltaic panels?

Main Hypothesis: The northern regions are likely to be the most suitable for the development of solar power plants.

Literature Review

Numerous studies have explored various aspects of solar energy utilization, some of which are summarized below.

Goodman et al. from Monash University in Australia, examined how Melbourne buildings could become self-sufficient by fully integrating solar energy systems. Their modeling ranged from individual buildings to entire neighborhoods and cities, revealing that, despite Melbourne's cloudy and rainy weather for about eight months a year, buildings could meet 74% of their electricity needs through the incorporation of solar technologies into roofs, walls, and windows. The study emphasized advancements in solar panel technology and its application in building facades, highlighting the benefits of solar window technology. Their detailed modeling considered density factors related to awnings and balconies, indicating that integrated solar solutions could

significantly enhance energy efficiency year-round. Linear regression analysis showed that densely populated urban centers, particularly commercial districts, had the highest potential for solar power integration (Goodman, Buxton, & Moloney, 2016).

(Shirinbakhsh & Harvey, 2024), in their research at the University of Toronto titled *Feasibility Study of Achieving Net Zero Energy Performance in Tall Buildings Using Solar Energy*, investigated the effectiveness of solar energy in tall buildings. They concluded that the geometry of the buildings and the types of solar cells used significantly affected energy efficiency. They found that achieving a net-zero energy balance solely through solar energy in tall buildings is challenging due to limited surface area for solar panels and the increasing density of urban populations. Their research focused on buildings over twenty stories tall, revealing that while roofs and facades can be equipped with solar panels, the optimal number of floors to maximize solar energy collection is ten or fewer (Shirinbakhsh & Harvey, 2024).

Ahadi et al. examined the feasibility of solar power plants in arid regions. Their descriptive-analytical study employed library and field data collection methods to assess various environmental parameters, including rainfall, sunshine hours, radiation levels, cloudiness, temperature, dust, frost, and altitude. They utilized GIS software alongside the Analytical Hierarchy Process (AHP) to analyze these data and identify suitable locations for solar energy development (Ahadi, Fakhrabadi, Pourshaghaghy, & Kowsary, 2023).

Hasanzadeh et al. investigated solar power plant siting using AHP and GIS techniques in their study on Ardabil. They highlighted the importance of expert-driven, multi-criteria decision-making models in identifying prime locations for solar facilities. Their analysis included twelve criteria spanning economic, environmental, and security dimensions, revealing that the most suitable land for solar plants was on the city outskirts, with significant correlations between site selection and distances from industrial zones, military areas, and transportation networks (Hasanzadeh, Kamran, Feizizadeh, & Mollabashi, 2023).

Tavakoli et al. conducted a feasibility assessment for a grid-connected photovoltaic power plant in Tehran's District 22. They noted that the growth of human societies correlates with energy production and consumption, emphasizing the environmental challenges posed by reliance on fossil fuels. Their study included an investigation of climatic conditions and the solar radiation potential of the site, selecting appropriate modules and inverters. They designed a power plant layout with 20 panels arranged in 82 rows, covering approximately 10,758 square meters, and used PVSyst software to optimize panel configuration and shading effects (Tavakolan & Nikoukar, 2022).

Shahin et al. addressed the multi-criteria solar power plant siting problem using a fuzzy Taguchi function in GIS for Kars province, Turkey. Their study underscored the importance of identifying suitable areas for solar energy development, considering that solar power and hydroelectricity are the primary renewable energy sources in the region. They modeled various indicators, such as altitude, slope, vegetation cover, and population density, using the fuzzy Taguchi method to determine optimal sites for solar power plants within the Kars city area (Sahin, Akkus, Koc, & van Sark, 2024).

In their article titled "Quantitative Study of the Influence of Urban Form on the Large-Scale Application of Rooftop Photovoltaics Using a Simple Method," (Li, Jing, Liu, & Zhao, 2021) explored the relationship between urban form and the potential for rooftop photovoltaic installation, aiming to promote low-carbon urban planning and reduce energy consumption. Their research analyzed 12 cities across China, representing various solar climates, and concluded that densely developed urban environments positively influence solar energy utilization. The study highlighted that large-scale implementation of rooftop photovoltaics is a promising strategy for renewable energy adoption and low-carbon urban development. Notably, it found that urban density significantly affects the feasibility of photovoltaic installations in cities located at high latitudes with moderate solar radiation, and this negative impact can be mitigated by lowering building heights (Li et al., 2021).

According to a report by the Clean Energy Council of Australia (2024), advances in building materials and construction techniques have facilitated the integration of solar energy in buildings. The efficiency of solar energy systems is largely determined by the amount of energy that can be captured and stored within a

structure, making building materials crucial. Various wall, floor, and roof coverings—from air cell blankets and reflective foils to steel and timber—play an important role in energy management. Additionally, building materials like core concrete blocks, double bricks, and sandstone contribute to maintaining comfortable indoor temperatures throughout the year. Insulation is also a critical factor in the efficiency of solar energy systems; high-quality insulation materials, such as cellulose, fiberglass, or spray foam, enhance heat retention from solar panels, thus boosting overall system performance (CleanEnergyCounci, 2024).

The Area under Study

The case study focuses on the coastal city of Tonekabon, specifically the Shiroodi and Islamabad neighborhoods. Tonekabon is located in the west of Mazandaran province along the Rasht-Chalos Road and has a population of 55,434 according to the 2016 census (Fig. 1).

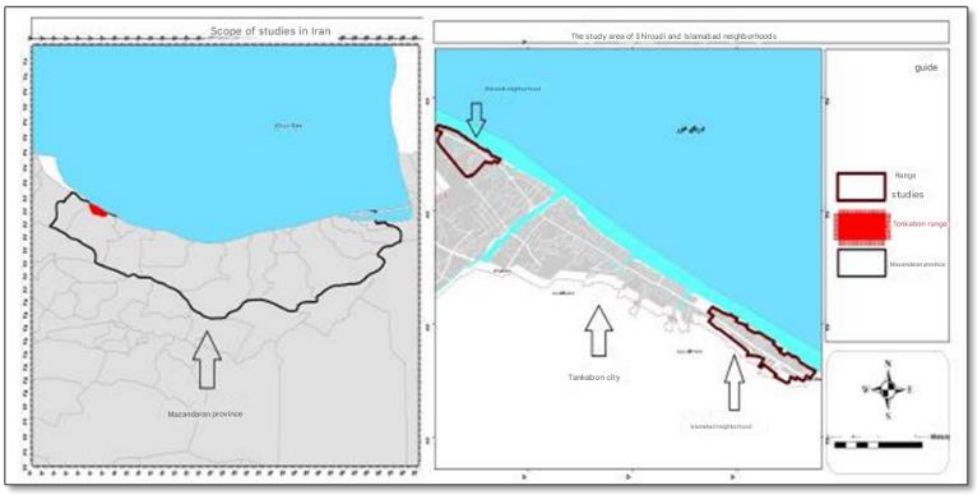

Figure 1. The Location of the Area under Study in the Mazandaran province

Methodology

This research is applied in nature and employs a descriptive-analytical method. Information was gathered through documentary studies, field observations, and questionnaires. Given the specialization of the topic, a total of 30 experts were selected as the target population, with 28 of them chosen as the sample using the Cochran formula to complete the questionnaires. Two methods were utilized in this study: the Inverse Hierarchy Analysis (IHWP) for site selection in GIS software and the PVsyst method for modeling the solar power plant.

The IHWP method consists of five steps:

1. **Determining the Data Matrix (Indices)**: Establishing the relevant indicators for analysis.
2. **Completing the Questionnaire**: Ranking the indicators and deducing their weight assumptions.
3. **Calculating Weights**: Determining the weights of the indicators based on the responses.
4. **Transferring Weights to GIS**: Inputting the calculated weights into GIS software for spatial analysis.
5. **Combining Maps**: Producing the final location map by integrating the various data layers.

Formulas:

$$j = D - (N - i)X \qquad X = \frac{D}{N}$$

- D=Score obtained from the Delphi model*D* =Score obtained from the Delphi model
- X=Initial score of each indicator*X*=Initial s core of each indicator
- j=Score obtained for different categories of each indicator*j*=Score obtained for different categories of each indicator
- N=Number of categories of each indicator*N* =Number of categories of each indicator
- i=Number assigned to different categories o f each indicator*i*=Number assigned to differ ent categories of each indicator

PVsyst is a comprehensive and user-friendly software tool designed for solar system analysis. It provides essential tools for studying, measuring, simulating, and analyzing

solar cell systems, making it valuable for architects, engineers, and researchers. The software includes a detailed help menu that explains the models and methods used, allowing users to assess how much solar energy can be converted into electricity in a specific area.

Results and Discussion

Location of Solar Power Plants in the Case Study Using the IHWP Method

Following the identification of relevant layers for determining the location of solar power plants, the selected indicators were ranked according to their significance through the Delphi method, which incorporates expert opinions. The inverse of each layer's rank then serves as its weight in the IHWP model. The final scores for various indicators and sub-indices are presented in Table 1.

Table 1: Weighting of Solar Power Plant Location Indicators in the Case Study

Indicator	Rank Based on Delphi	Inverse Rank	Number of Classes per Indicator	Classification				
Population Density (per hectare)	1	8	4	Less than 100	Between 100 and 120	Between 120 and 140	Above 140	
				2	4	6	8	
Accessibility to Communication Network	2	7	5	Less than 30 meters	Above 120 meters	Between 100 and 120 meters	Between 60 and 100 meters	Between 30 and 60 meters
				1.4	1.4	4.2	5.6	7
Distance from Rivers and Sea	3	6	5	Less than 200 meters	Between 200 and 300 meters	Between 300 and 400 meters	Between 400 and 500 meters	Above 500 meters
				1.2	2.4	3.6	4.8	6
Access to Sparse and Abandoned Lands	4	5	5	Less than 50 meters	Between 50 and 100 meters	Between 100 and 150 meters	Between 150 and 200 meters	Above 200 meters
				5	4	3	2	1
Building Density	5	4	3	Less than 50%	Between 50 and 60	Above 60		
				1.3	2.7	4		
Distance from Farms and Gardens	6	3	5	Less than 50 meters	Between 50 and 80 meters	Between 80 and 100 meters	Between 100 and 120 meters	Above 120 meters
				0.6	1.2	1.8	2.4	3
Distance from Industries	7	2	5	Less than 50 meters	More than 200 meters	Between 150 and 200 meters	Between 100 and 150 meters	Between 50 and 100 meters
				0.4	0.8	1.2	1.6	2
Average Area of Lots	8	1	5	Less than 1000 sq m	Above 4000 sq m	Between 1000 and 2000 sq m	Between 2000 and 3000 sq m	Between 3000 and 4000 sq m
				0.2	0.4	0.6	0.8	1

Using the Raster Calculate tool, we combined the score columns from each information layer created in the GIS environment. This process produced a final map that classifies the data into five distinct categories (very low, low, medium, high, and very high) regarding suitable locations for solar power plants in the case study area. In Map (2), weighted layers are displayed, where red represents very unfavorable locations and blue indicates very favorable locations.

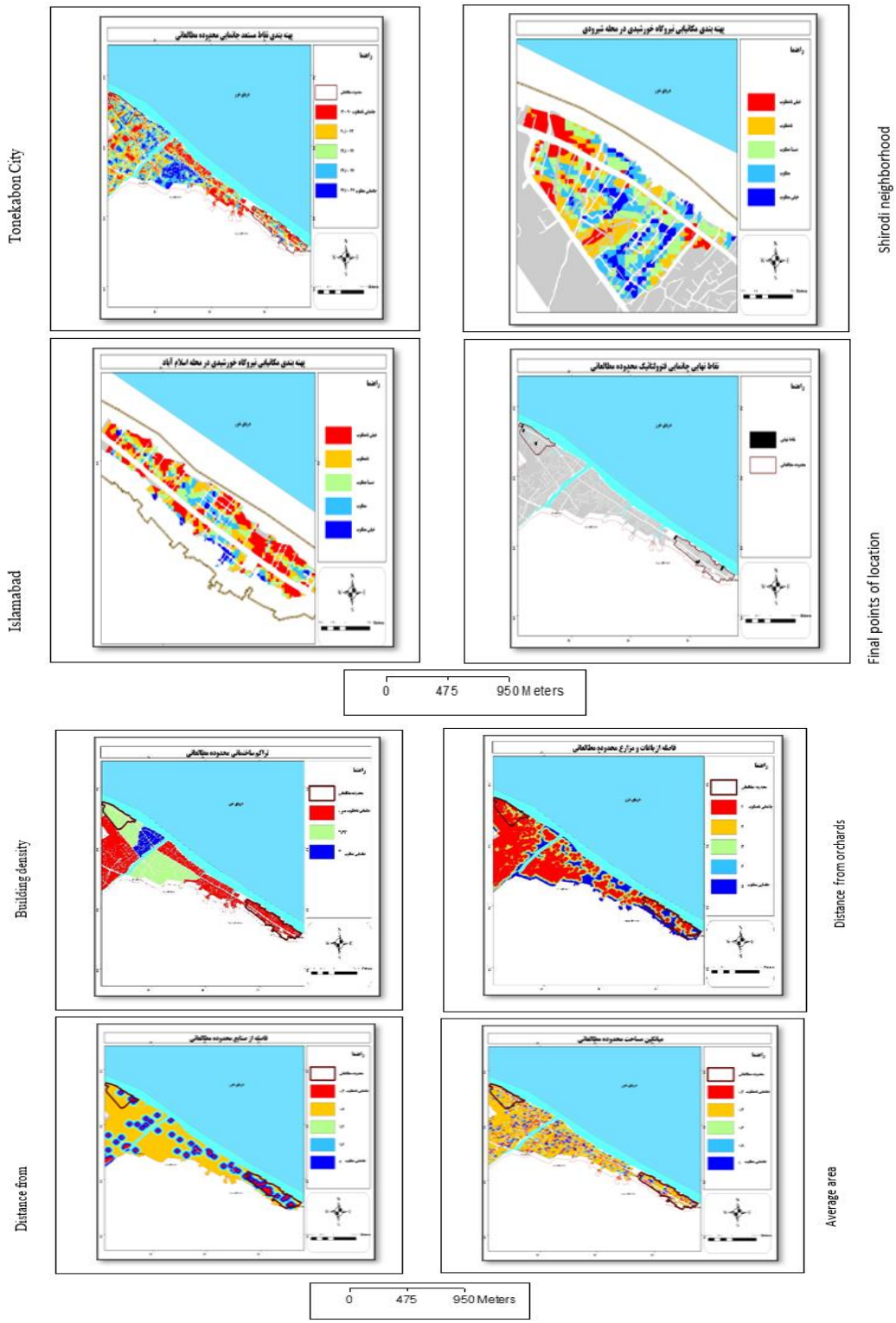

Figure 2. Steps for modeling information layers using the IHWP method in a GIS environment

The zoning for solar power plant locations in Tonekabon city is as follows: 26% of the city falls into a very unfavorable zone, 23% into an unfavorable zone, 20% is relatively suitable, another 20% is suitable, and 11% is completely suitable, primarily located in the city's central area. The Islamabad neighborhood shows greater potential for solar power plant construction, with favorable areas concentrated 72.88% in the central region and 27.11% in the southern area of the Shirodi neighborhood.

Table 2: Final Locations for Solar Power Plants in the Shiroodi and Islamabad Neighborhoods of Tonekabon City

Neighborhood	Map Code	Area	Longitude	Latitude
Islamabad	1	3178	493867.3	4071589.5
Islamabad	2	3223	493842.1	4071601
Shiroodi	10	3672	484711.2	4076248.7
Islamabad	26	3509	493052.7	4071789.8
Islamabad	27	2572	493100.1	4071817.5
Islamabad	50	2829	492354	4072590.5
Islamabad	51	2874	492335.7	4072601.2
Shiroodi	54	3922	487848.2	4075671.1
Shiroodi	57	3553	487443.7	4076096.7

Table 3: Final Ranking of Top License Plates

Identification Number 54 (Shiroodi Neighborhood)	First Place
Identification Numbers 26 and 27 (Islamabad Neighborhood)	Second Place
Identification Number 57 (Shiroodi Neighborhood)	Third Place
Identification Numbers 50 and 51 (Islamabad Neighborhood)	Fourth Place
Identification Numbers 1 and 2 (Islamabad Neighborhood)	Fifth Place
Identification Number 10 (Shiroodi Neighborhood)	Sixth Place

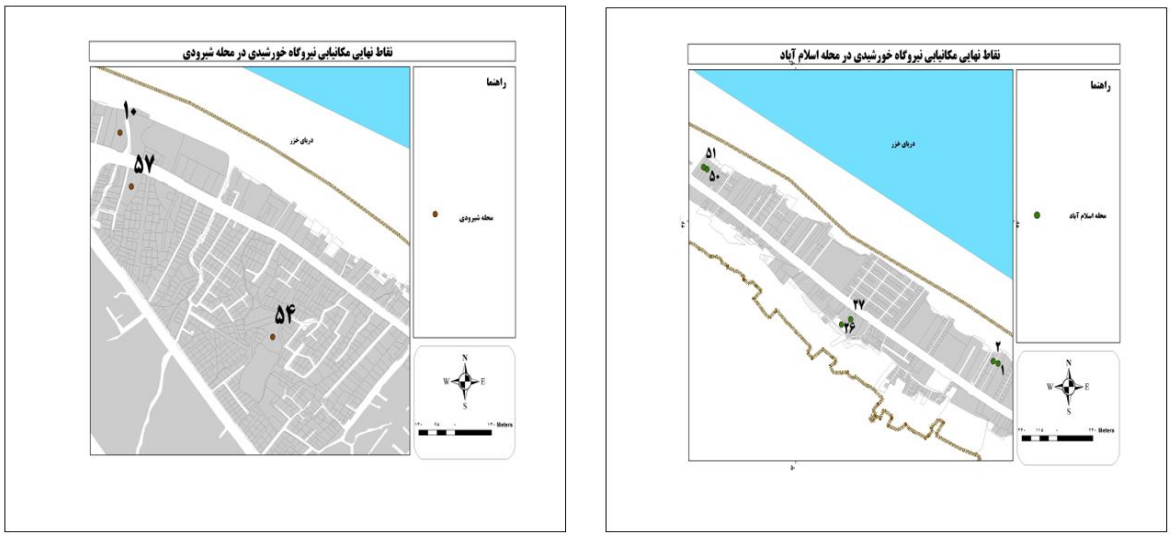

Figure 3. Final points for locating solar power plants in the case study

Prioritizing Selected Locations for Solar Power Plant Construction Using the PV Sys Method

At this stage, we focused on the highest-ranking locations in the Islamabad neighborhood. Three geographical sites—corresponding to plates 1+2, 51+50, and 26+27—were evaluated. The locations, along with the area analyzed for electricity supply, are illustrated in Map (4). In this specified area, the electricity requirements for 150 residential units, a mosque (with two loudspeakers), and two shops total 1,327,396 Wh/day.

Table (4) outlines both the total electricity demand and the hourly breakdown of this

consumption, highlighting peak usage hours from 5 PM to 12 AM. To assess how the area (number of solar panels) affects the power plant's performance, modeling was conducted for three areas of 3,000, 4,000, and 5,000 square meters across the three selected sites. The results of this modeling were then compared. For this study, only location 26+27 in the Islamabad neighborhood, which ranked second, was considered.

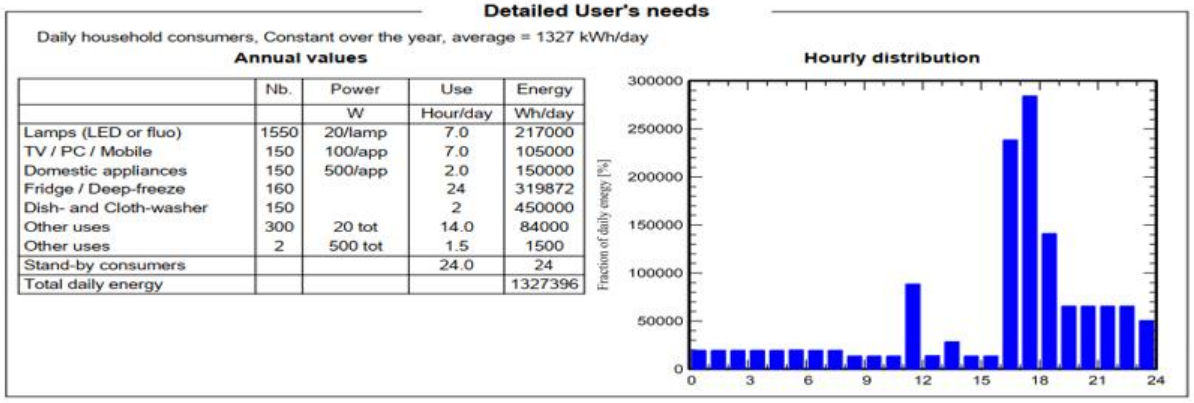

Detailed User's needs

Daily household consumers, Constant over the year, average = 1327 kWh/day

Annual values

	Nb.	Power	Use	Energy
		W	Hour/day	Wh/day
Lamps (LED or fluo)	1550	20/lamp	7.0	217000
TV / PC / Mobile	150	100/app	7.0	105000
Domestic appliances	150	500/app	2.0	150000
Fridge / Deep-freeze	160		24	319872
Dish- and Cloth-washer	150		2	450000
Other uses	300	20 tot	14.0	84000
Other uses	2	500 tot	1.5	1500
Stand-by consumers			24.0	24
Total daily energy				1327396

Modeling of Plates 26+27, 3000 Square Meters: In Map (5), the position of the plates is input into the PVsyst software. The power plant is initially set to cover an area of 3,000 square meters, containing 10,800 panels configured in 30 series rows and 360 parallel rows, resulting in a total panel area of 2,527 square meters. Figure 5 displays the specifications for the panels, batteries, and the surface area of the panels.

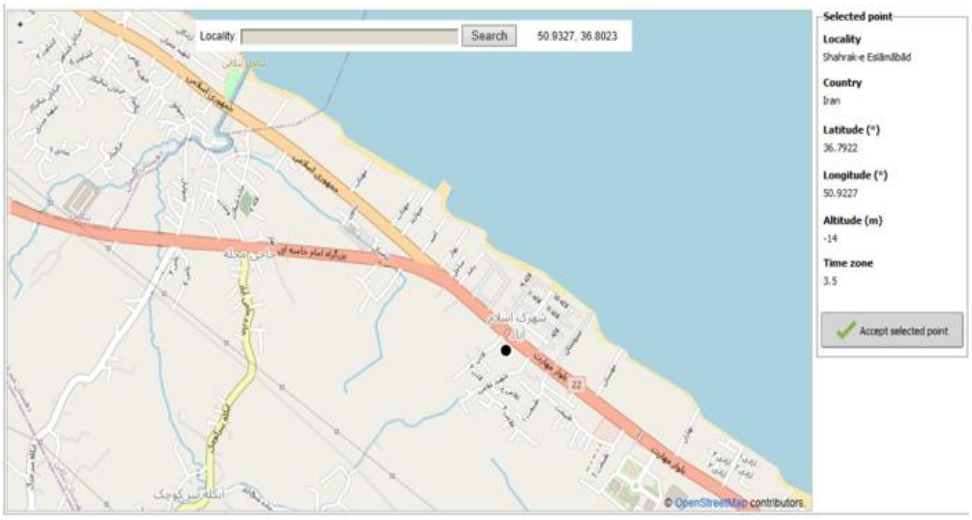

Figure 5. Location of No. 26+27

As illustrated in Figure (1), the solar fraction is less than one during the first two months and the last month of the year, indicating that the power plant fails to meet total electricity demands during these periods, necessitating the use of an auxiliary power source. In contrast, the solar fraction equals one during the remaining months, showing that the power plant generates enough electricity to meet all requirements.

Interestingly, system performance is higher in the first two and last two months of the year than in the other months. This variation occurs because, in the hotter months, electricity production exceeds demand, leading to excess energy waste. To enhance the power plant's efficiency during these hotter months, reducing the number of panels could be a viable option. Figure (2) further illustrates the loss rates across different system components, revealing that loss rates are significantly higher during the hotter months compared to the cooler months

.

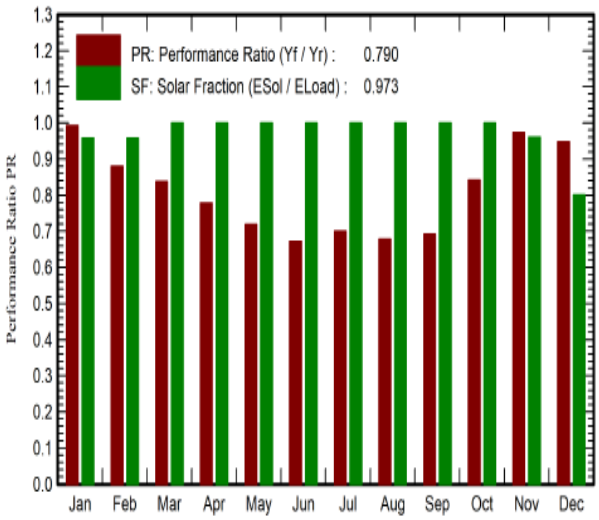

Chart 1: Solar fraction and system performance

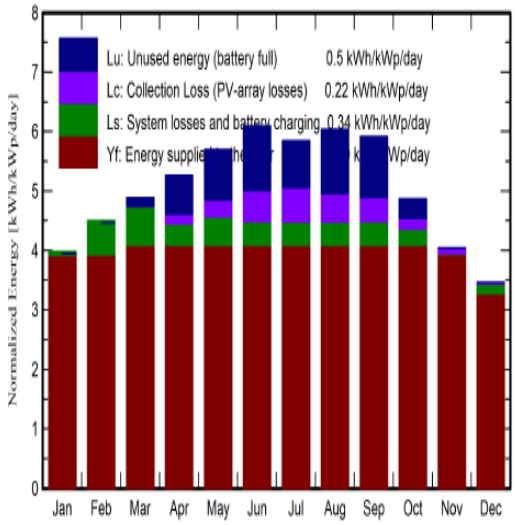

Chart 2: Casualty rate

Figure 3 illustrates the average temperature of the panel surface, showing that the temperature rises with increasing solar radiation. Figure 4 presents the energy output of the panel in relation to solar radiation, indicating that energy production increases as solar radiation intensifies. However, when solar radiation surpasses a certain threshold, the energy output stabilizes at a constant level.

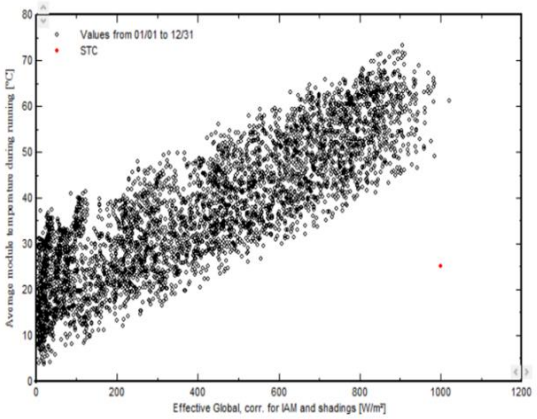

Figure 3: Average Temperature of the Panel Surface

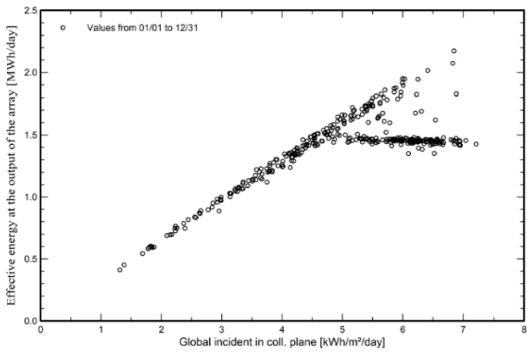

Figure 4: Energy Output in Relation to Solar Radiation

Table (5) summarizes the results, revealing that the solar fraction during the first and last months of the year is less than one. This indicates that the power plant does not meet the total electricity demand during these months, primarily due to lower solar radiation and the angle of incidence. Conversely, in the remaining months, the power plant successfully supplies the total electricity required by consumers.

Table 5: Summary of results.

	GlobHor kWh/m²	GlobEff kWh/m²	E_Avail kWh	EUnused kWh	E_Miss kWh	E_User kWh	E_Load kWh	SolFrac ratio
January	71.9	120.4	38383	0	1735	39415	41149	0.958
February	84.8	122.6	39189	0	1541	35626	37167	0.959
March	121.2	148.2	47095	1451	0	41149	41149	1.000
April	147.3	153.8	47700	6287	0	39822	39822	1.000
May	185.4	171.5	52530	8538	0	41149	41149	1.000
June	202.5	177.2	52305	10501	0	39822	39822	1.000
July	195.9	175.8	51045	7900	0	41149	41149	1.000
August	182.3	182.3	53971	10810	0	41149	41149	1.000
September	149.1	173.1	51680	9889	0	39822	39822	1.000
October	108.5	148.1	45394	3265	0	41149	41149	1.000
November	74.4	119.1	36787	0	1587	38235	39822	0.960
December	62.0	105.5	33071	0	8223	32926	41149	0.800
Year	1585.4	1797.6	549150	58641	13086	471413	484500	0.973

Legends

GlobHor	Global horizontal irradiation
GlobEff	Effective Global, corr. for IAM and shadings
E_Avail	Available Solar Energy
EUnused	Unused energy (battery full)
E_Miss	Missing energy
E_User	Energy supplied to the user
E_Load	Energy need of the user (Load)
SolFrac	Solar fraction (EUsed / ELoad)

Modeling of Plates 26+27, 4000 Square Meters:

In this model, the power plant covers an area of 4,000 square meters and consists of 14,100 panels, configured in 30 series rows and 470 parallel rows. The total area occupied by the panels is 3,299 square meters. As shown in Figure (5), the solar fraction is equal across all months of the year, indicating that the power plant meets the total electricity demand. However, system performance is low due to losses. To enhance system efficiency, the number of panels may be reduced. Figure (6) illustrates the loss rates of different components within the system, with higher losses observed during the warmer months compared to the colder months.

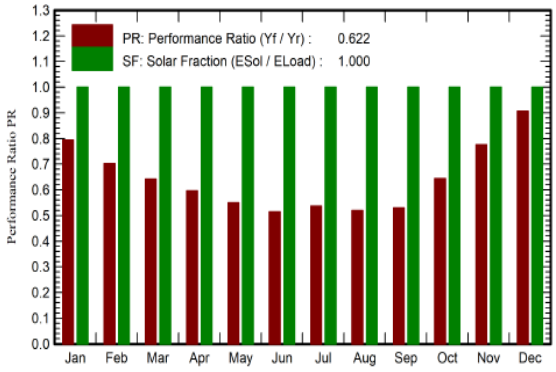

Figure 5: Solar Fraction and System Performance

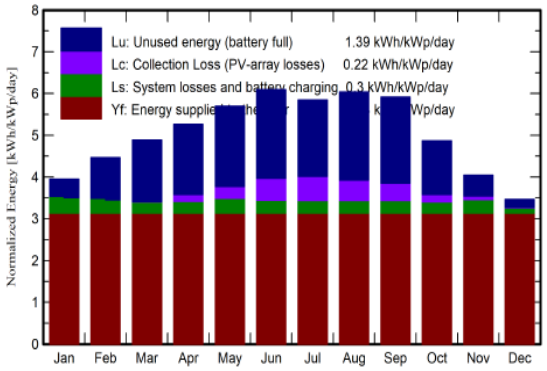

Figure 6: Loss Rate

Figure (7) displays the average temperature of the panel surface. The data indicates that the average temperature increases with solar radiation. Figure (8) shows the energy output from the panels as a function of solar radiation, revealing that energy production rises with increasing solar radiation. When solar radiation exceeds a specific threshold, the energy output stabilizes at a constant value.

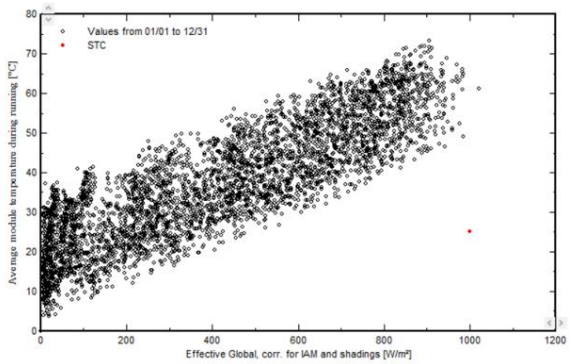

Figure 7: Average Temperature of the Panel Surface

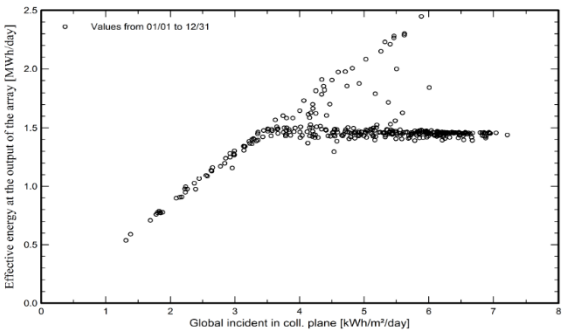

Figure 8: Energy Output in Relation to Solar Radiation

Table (6) summarizes the results, showing that the solar fraction remains at one throughout the year, confirming that the power plant supplies the total electricity required.

Table 6: Summary of Results

	GlobHor kWh/m²	GlobEff kWh/m²	E_Avail kWh	EUnused kWh	E_Miss kWh	E_User kWh	E_Load kWh	SolFrac ratio
January	71.9	120.4	50367	5808	0.000	41149	41149	1.000
February	84.8	122.6	51664	11966	0.000	37167	37167	1.000
March	121.2	148.2	62253	19387	0.000	41149	41149	1.000
April	147.3	153.8	62823	21286	0.000	39822	39822	1.000
May	185.4	171.5	69157	25257	0.000	41149	41149	1.000
June	202.5	177.2	68784	26941	0.000	39822	39822	1.000
July	195.9	175.8	67192	23971	0.000	41149	41149	1.000
August	182.3	182.3	70981	27719	0.000	41149	41149	1.000
September	149.1	173.1	68012	26158	0.000	39822	39822	1.000
October	108.5	148.1	59787	16859	0.000	41149	41149	1.000
November	74.4	119.1	48339	6201	0.000	39822	39822	1.000
December	62.0	105.5	43286	2408	0.000	41149	41149	1.000
Year	1585.4	1797.6	722646	213962	0.000	484500	484500	1.000

Legends

GlobHor	Global horizontal irradiation
GlobEff	Effective Global, corr. for IAM and shadings
E_Avail	Available Solar Energy
EUnused	Unused energy (battery full)
E_Miss	Missing energy
E_User	Energy supplied to the user
E_Load	Energy need of the user (Load)
SolFrac	Solar fraction (EUsed / ELoad)

Modeling of Plates 26+27, 5000 Square Meters:

In this model, the power plant spans 5,000 square meters and includes 17,400 panels, arranged in 30 series rows and 580 parallel rows, with a total panel area of 4,072 square meters. Similar to the previous model, Figure (9) indicates that the solar fraction remains consistent across all months, signifying that the power plant meets total electricity requirements. However, system performance is hindered by losses, and reducing the number of panels could improve efficiency. Figure (10) again represents the loss rates in various parts of the system, with higher rates during the warmer months.

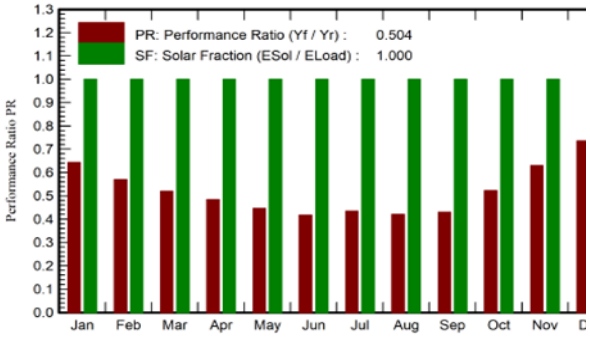

Figure 9: Solar Fraction and System Performance

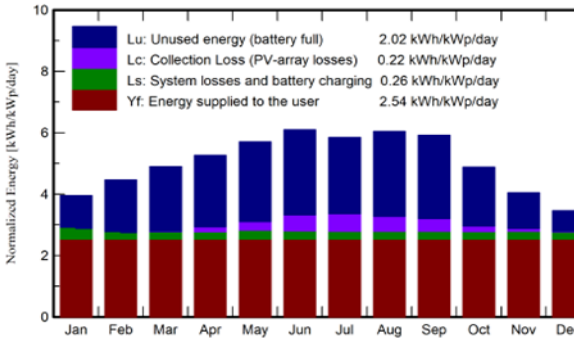

Figure 10: Loss Rate

Figure (11) illustrates the average temperature of the panel surface, which increases with rising solar radiation. Figure (12) shows the energy output from the panels as solar radiation increases, indicating that output increases until it reaches a constant value when radiation exceeds a certain limit.

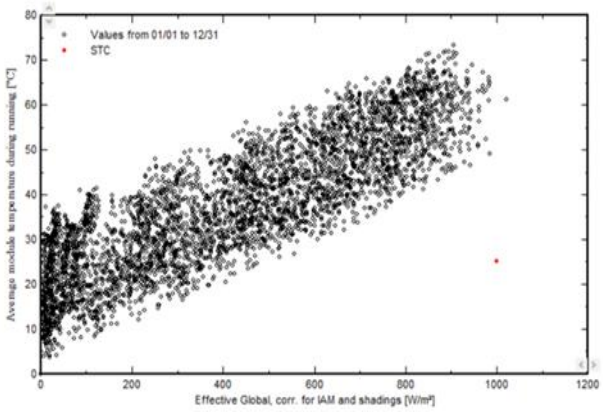

Figure 11: Average Temperature of the Panel Surface

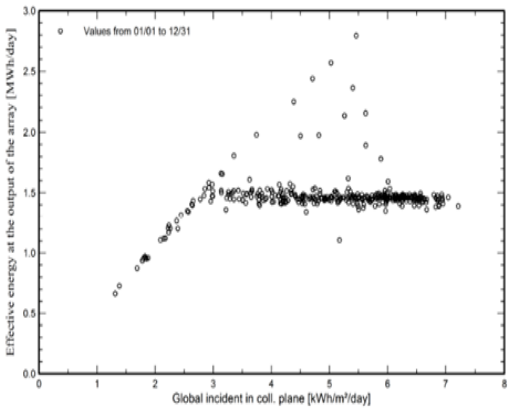

Figure 12: Energy Output in Relation to Solar Radiation

Table (7) offers a summary of the results, confirming that the solar fraction equals one throughout the year, indicating that the power plant meets total electricity demands.

Table 7: Summary of Results

	GlobHor kWh/m²	GlobEff kWh/m²	E_Avail kWh	EUnused kWh	E_Miss kWh	E_User kWh	E_Load kWh	SolFrac ratio
January	71.9	120.4	62576	17206	0.000	41149	41149	1.000
February	84.8	122.6	64143	25125	0.000	37167	37167	1.000
March	121.2	148.2	77242	34088	0.000	41149	41149	1.000
April	147.3	153.8	77937	36419	0.000	39822	39822	1.000
May	185.4	171.5	85758	41967	0.000	41149	41149	1.000
June	202.5	177.2	85276	43374	0.000	39822	39822	1.000
July	195.9	175.8	83356	40073	0.000	41149	41149	1.000
August	182.3	182.3	88010	44701	0.000	41149	41149	1.000
September	149.1	173.1	84345	42460	0.000	39822	39822	1.000
October	108.5	148.1	74170	30909	0.000	41149	41149	1.000
November	74.4	119.1	60056	18072	0.000	39822	39822	1.000
December	62.0	105.5	53784	10958	0.000	41149	41149	1.000
Year	1585.4	1797.6	896654	385353	0.000	484500	484500	1.000

Legends

GlobHor	Global horizontal irradiation
GlobEff	Effective Global, corr. for IAM and shadings
E_Avail	Available Solar Energy
EUnused	Unused energy (battery full)
E_Miss	Missing energy
E_User	Energy supplied to the user
E_Load	Energy need of the user (Load)
SolFrac	Solar fraction (EUsed / ELoad)

Investigation of Plates 10, 57, and 54 in Karimabad Neighborhood:

Three geographic locations—corresponding to plates 10, 57, and 54—have been assessed in the Karimabad neighborhood, as shown in Map (6). Modeling has been performed for a 10-story building, which requires 128,296 Wh/day. Table (8) summarizes both the total electricity demand and the hourly breakdown, with peak consumption occurring from 5 PM to 12 AM.

To evaluate the impact of area (and consequently the number of panels) on power plant performance, simulations were conducted for three areas of 200 and 300 square meters across the three mentioned geographic locations, comparing the results. Aerial data, similar to that of the Islamabad neighborhood, has been used for this analysis. Notably, plate 54 has been identified as the top-ranked option.

Map 6: Geographical Location of Karimabad Neighborhood

Table 8: Total Electricity Requirements and Hourly Breakdown

Detailed User's needs

Daily household consumers, Constant over the year, average = 128 kWh/day

Annual values

	Nb.	Power	Use	Energy
		W	Hour/day	Wh/day
Lamps (LED or fluo)	12	20/lamp	7.0	1680
TV / PC / Mobile	30	100/app	7.0	21000
Domestic appliances	50	500/app	2.0	50000
Fridge / Deep-freeze	10		24	19992
Dish- and Cloth-washer	10		2	30000
Other uses	20	20 tot	14.0	5600
Stand-by consumers			24.0	24
Total daily energy				128296

Hourly distribution

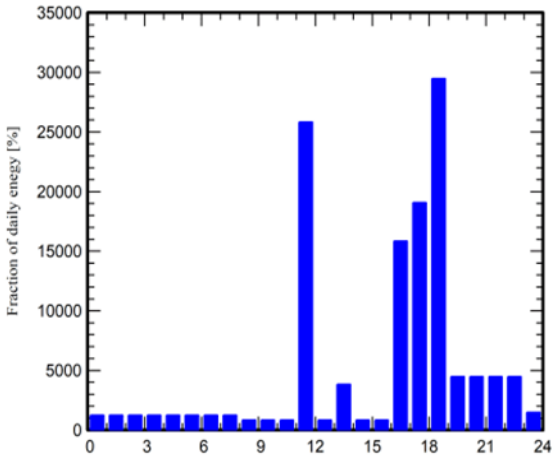

Modeling Karimabad Lot 54, 200 Square Meters:

In Map (7), the location of Lot 54 is input into the PV System photovoltaic software. The power plant covers an area of 200 square meters and includes 800 panels, configured in 20 series rows and 40 parallel rows, with a total panel area of 187 square meters. As shown in Figure (13), the solar fraction is less than one throughout the year. This indicates that during months when the solar fraction is below one, the power plant does not supply the total electricity demand and requires an auxiliary power source. The system performance exceeds the solar fraction, as the electricity produced is used immediately, resulting in reduced losses. However, during the hot months of the year, system performance declines due to higher losses. Figure (14) displays the loss rates in different components of the system, highlighting that losses are greater in the warmer months compared to the colder months.

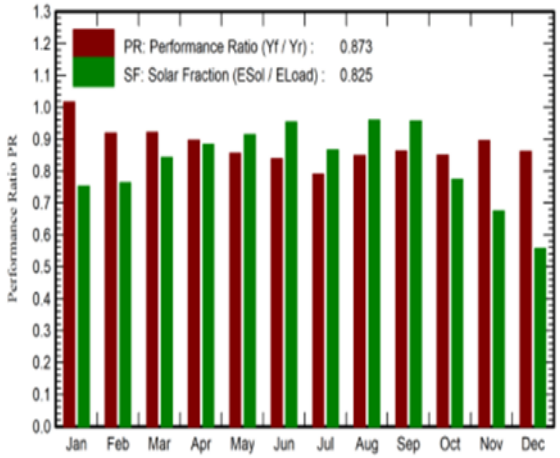

Figure 13: Solar Fraction and System Performance

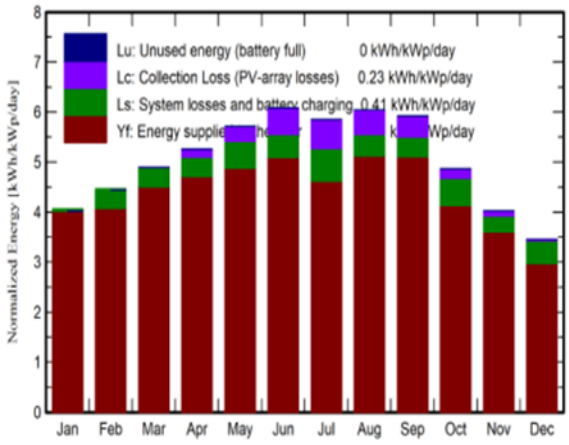

Figure 14: Loss Rate

Figure (15) illustrates the average temperature of the panel surface, which increases with rising solar radiation. Additionally, Figure (16) shows the energy output from the panels as a function of solar radiation, indicating that energy production increases consistently without reaching a plateau.

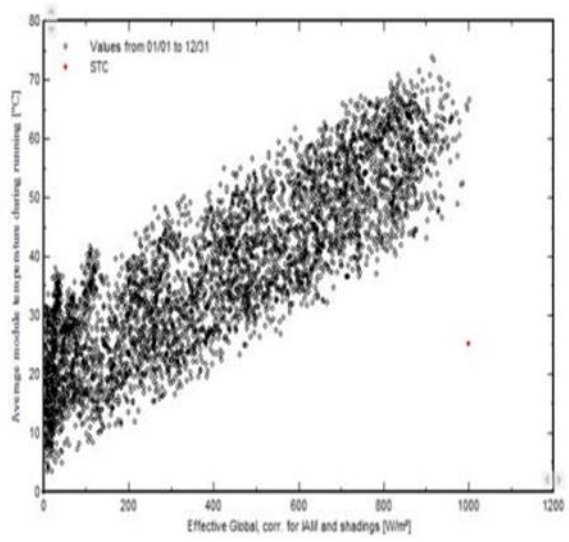

Figure 15: Average Temperature of the Panel Surface

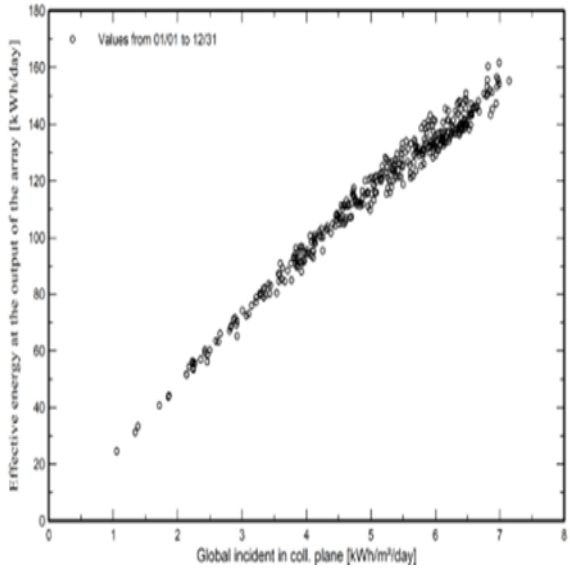

Figure 16: Energy Output in Relation to Solar Radiation

Table (9) provides a summary of results, indicating that the solar fraction is below one in the first and last months of the year, meaning the power plant does not meet electricity demands during any month. Moreover, electricity consumption exceeds production throughout the year.

Table 9: Summary of Results

	GlobHor kWh/m²	GlobEff kWh/m²	E_Avail kWh	EUnused kWh	E_Miss kWh	E_User kWh	E_Load kWh	SolFrac ratio
January	71.9	120.6	2855	0.000	985	2992	3977	0.752
February	84.8	122.1	2875	0.062	851	2741	3592	0.763
March	121.2	148.3	3491	0.130	624	3353	3977	0.843
April	147.3	153.8	3517	0.000	449	3400	3849	0.883
May	185.4	171.9	3859	0.028	343	3634	3977	0.914
June	202.5	176.9	3827	0.000	177	3672	3849	0.954
July	195.9	176.1	3754	0.081	534	3443	3977	0.866
August	182.3	182.4	3962	0.026	163	3814	3977	0.959
September	149.1	173.4	3797	0.016	167	3681	3849	0.957
October	108.5	148.0	3341	0.119	900	3077	3977	0.774
November	74.4	118.7	2710	0.026	1252	2597	3849	0.675
December	62.0	105.4	2441	0.074	1763	2214	3977	0.557
Year	1585.4	1797.7	40431	0.561	8209	38619	46828	0.825

Legends

GlobHor	Global horizontal irradiation
GlobEff	Effective Global, corr. for IAM and shadings
E_Avail	Available Solar Energy
EUnused	Unused energy (battery full)
E_Miss	Missing energy
E_User	Energy supplied to the user
E_Load	Energy need of the user (Load)
SolFrac	Solar fraction (EUsed / ELoad)

Karimabad Lot 54, 300 Square Meters:

In this model, the power plant occupies an area of 300 square meters and consists of 1,200 panels, arranged in 20 series rows and 60 parallel rows, with a total panel area of 281 square meters.

As depicted in Figure (17), the solar fraction is equal across all months, signifying that the power plant successfully meets total electricity requirements. However, system performance remains low due to losses, and reducing the number of panels could improve efficiency. Figure (18) illustrates the loss rates in various parts of the system, again showing that losses are higher during the warmer months compared to the cooler months.

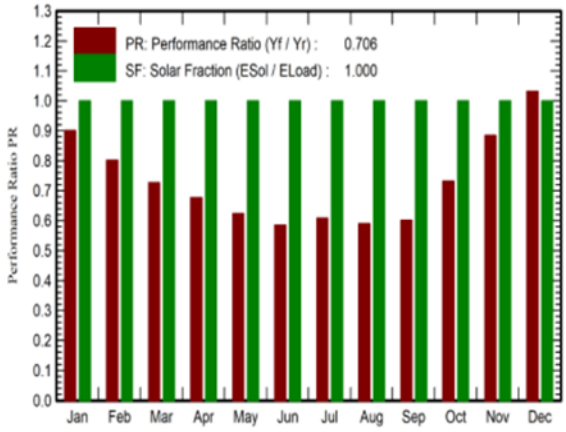

Figure 17: Solar Fraction and System Performance

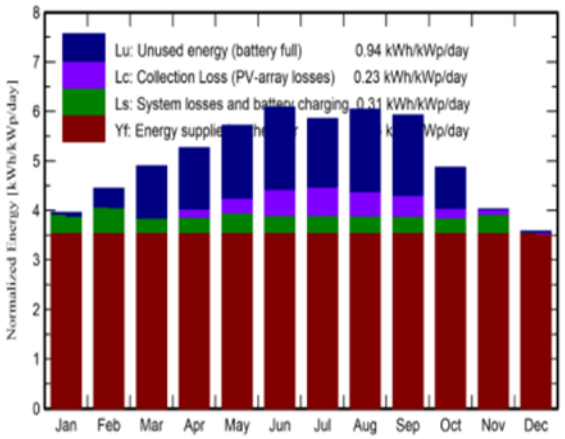

Figure 18: Loss Rate

Figure (19) depicts the average temperature of the panel surface, which rises with increasing solar radiation. Figure (20) shows the energy output from the panels in relation to solar radiation, demonstrating that energy output increases as solar radiation rises, remaining consistent only after a certain threshold.

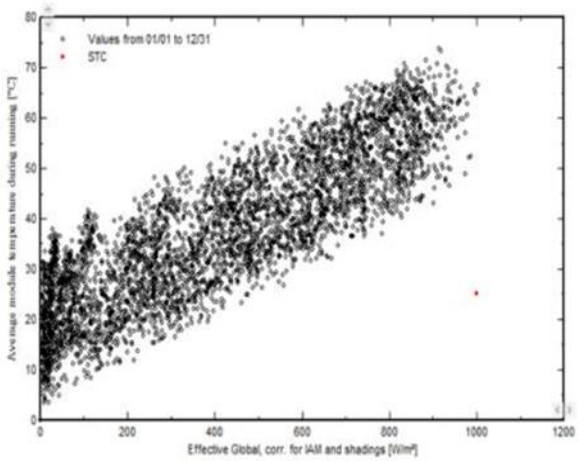

Figure 19: Average Temperature of the Panel Surface

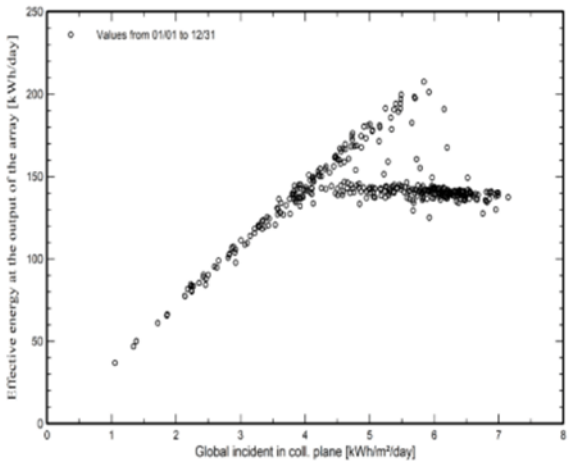

Figure 20: Energy Output in Relation to Solar Radiation

Table (10) summarizes the results, confirming that the solar fraction is one for all months, indicating that the power plant has provided the total electricity required throughout the year.

Table 10: Summary of Results

	GlobHor kWh/m²	GlobEff kWh/m²	E_Avail kWh	EUnused kWh	E_Miss kWh	E_User kWh	E_Load kWh	SolFrac ratio
January	71.9	120.6	2856	0.000	984	2993	3977	0.753
February	84.8	122.1	2875	0.062	851	2741	3592	0.763
March	121.2	148.3	3491	0.130	624	3353	3977	0.843
April	147.3	153.8	3517	0.000	449	3400	3849	0.883
May	185.4	171.9	3859	0.028	343	3634	3977	0.914
June	202.5	176.9	3827	0.000	177	3672	3849	0.954
July	195.9	176.1	3754	0.081	534	3443	3977	0.866
August	182.3	182.4	3962	0.026	163	3815	3977	0.959
September	149.1	173.4	3797	0.016	167	3681	3849	0.957
October	108.5	148.0	3341	0.119	900	3077	3977	0.774
November	74.4	118.7	2711	0.026	1252	2597	3849	0.675
December	62.0	105.4	2441	0.074	1763	2214	3977	0.557
Year	1585.4	1797.7	40432	0.561	8208	38620	46828	0.825

Legends

GlobHor	Global horizontal irradiation
GlobEff	Effective Global, corr. for IAM and shadings
E_Avail	Available Solar Energy
EUnused	Unused energy (battery full)
E_Miss	Missing energy
E_User	Energy supplied to the user
E_Load	Energy need of the user (Load)
SolFrac	Solar fraction (EUsed / ELoad)

Conclusion

The advancement of renewable energy is a key indicator of economic development, showcasing significant benefits across economic, social, cultural, environmental, and organizational dimensions. In recent years, factors such as the global energy crisis, dwindling fossil fuel resources, rising greenhouse gas emissions, and escalating global temperatures have underscored the importance of renewable energy sources, particularly solar energy. This shift has led to

increased interest in solar power not only for large-scale public utilities but also for residential use.

Various solar power plants have been designed, constructed, and commissioned, generating over a thousand kilowatts of electricity daily through numerous projects. This study examined the feasibility of solar power plant locations using eight criteria: population density, access to communication networks, proximity to rivers and seas, availability of barren or abandoned land, building density, distance from farms and orchards, distance from industrial areas, and average plot size. The case study focused on the Shiroodi and Islamabad neighborhoods in Tonekabon city.

The research analysis consisted of two parts. In the first part, the IHWP method was applied within GIS software to determine suitable locations for solar power plants. The findings indicate the following:

1. **Land Suitability**: Approximately 26% of the city area is classified as very unsuitable for solar development, 23% as unsuitable, 20% as relatively suitable, 20% as suitable, and 11% as completely suitable. Most of the optimal areas are located in the central part of the city. This result contradicts the initial research hypothesis, which suggested that the northern regions would be more suitable.
2. **Neighborhood Comparison**: The Islamabad neighborhood presents more potential for solar power plant development than the Shiroodi neighborhood. Specifically, 72.88% of the central area in Islamabad is favorable for solar plants, compared to 27.11% in the southern area of Shiroodi.

Additionally, modeling results using PVsyst software revealed that geographic location in the Karimabad region does not significantly influence solar fraction and system performance. However, increasing the area of the power plant from 200 square meters to 300 square meters improves the solar fraction, though system performance decreases. The highest solar fraction of 100% was observed for a power plant with an area of 300 square meters, indicating that this configuration delivers optimal performance in Karimabad.

In the Islamabad region, geographic location also does not significantly affect solar fraction and system performance. Increasing the power plant area to 4,000 square meters results in a solar fraction of 100%, but system performance declines. Even at 5,000 square meters, the solar fraction remains at 100%, yet system performance continues to decrease. Thus, establishing a power plant with an area of 4,000 square meters in the Islamabad region is recommended for the best performance.

References

Ahadi, P., Fakhrabadi, F., Pourshaghaghy, A., & Kowsary, F. (2023). Optimal site selection for a solar power plant in Iran via the Analytic Hierarchy Process (AHP). *Renewable Energy, 215*, 118944.

Ahmadian, E. (2021). *Impact of Urban Built Form and Urban Density on Building Energy Performance in Different Climates.* University of Lincoln,

Ajiboye, A., Agboola, D., Atayese, M., & Kadiri, M. (2011). Some Aspect of Dormancy Studies and Vitamin D Content of Four Tree Seed Species. *International Research Journal of Plant Science, 2*(2), 32–36.

Alghoul, S. K., Rijabo, H. G., & Mashena, M. E. (2017). Energy consumption in buildings: A correlation for the influence of window to wall ratio and window orientation in Tripoli, Libya. *Journal of Building Engineering, 11*, 82–86.

CleanEnergyCounci. (2024). Clean Energy Council releases Clean Energy Australia 2024 report. Retrieved from https://cleanenergycouncil.org.au/news-resources/clean-energy-australia-2024-report

Goodman, R., Buxton, M., & Moloney, S. (2016). *Planning Melbourne: Lessons for a sustainable city*: CSIRO PUBLISHING.

Hasanzadeh, M., Kamran, K. V., Feizizadeh, B., & Mollabashi, S. H. (2023). Land suitability analysis for solar power plant using satellite imagery processing and GIS, Ardabil, Iran.

Hassaan, M. A., Hassan, A., & Al-Dashti, H. (2021). GIS-based suitability analysis for siting solar power plants in Kuwait. *The Egyptian Journal of Remote Sensing and Space Science, 24*(3), 453–461.

Khajavipour, A., Shahraki, M. R., & Hosseinzadeh Saljooghi, F. (2021). Evaluation of the Effective Factors in Locating a Photovoltaic Solar Power Plant Using Fuzzy Multi-Criteria Decision-Making Method. *Journal of Renewable Energy and Environment, 8*(3), 16–25.

Kumar, R., Rajoria, C., Sharma, A., & Suhag, S. (2021). Design and simulation of standalone solar PV system using PVsyst Software: A case study. *Materials Today: Proceedings, 46*, 5322–5328.

Li, Y., Jing, K., Liu, F., & Zhao, F. (2021). A Quantitative Study of the Influence of Urban Form on Large-Scale Application of Rooftop Photovoltaics Using Simplified Method. *International Journal of Sustainable and Green Energy*, *10*(2), 63.

Nandini, K., Jayalakshmi, N., & Jadoun, V. K. (2024). A combined approach to evaluate power quality and grid dependency by solar photovoltaic based electric vehicle charging station using hybrid optimization. *Journal of Energy Storage*, *84*, 110967.

Rana, M. S. P., & Moniruzzaman, M. (2024). Demarcation of suitable site for solar photovoltaic power plant installation in Bangladesh using geospatial techniques. *Next Energy*, *3*, 100109.

Sahin, G., Akkus, I., Koc, A., & van Sark, W. (2024). Multi-criteria solar power plant siting problem solution using a GIS-Taguchi loss function based interval type-2 fuzzy approach: The case of Kars Province/Turkey. *Heliyon*, *10*(10).

Shirinbakhsh, M., & Harvey, L. D. (2024). Feasibility of achieving net-zero energy performance in high-rise buildings using solar energy. *Energy and Built Environment*, *5*(6), 946–956.

Tavakolan, M., & Nikoukar, S. (2022). Developing an optimization financing cost-scheduling trade-off model in construction project. *International Journal of Construction Management*, *22*(2), 262–277.

Wei, L. J., Islam, M., Hasanuzzaman, M., & Cuce, E. (2024). Energy consumption, power generation and performance analysis of solar photovoltaic module based building roof. *Journal of Building Engineering*, *90*, 109361.

Zhang, M., Xu, L., & Liu, F. (2024). Batch preparation and characterization of zein-based beaded nanofiber membranes for active food packaging. *International Journal of Biological Macromolecules*, *276*, 133966.